Catalyst Luminescence Exploited as an Inherent In Situ Probe of Photoredox Catalysis

David J. Hayne+,[a] Sudip Mohapatra+,[a, e] Joseph C. Bawden,[a] Jacqui L. Adcock,[a] Gregory J. Barbante,[a, f] Egan H. Doeven,[b] Catherine L. Fraser,[a] Timothy U. Connell,[a, g] Jonathan M. White,[c] Luke C. Henderson,*[d] and Paul S. Francis*[a]

The luminescence of commonly used photoredox catalysts offers a continuous inherent in situ probe of electron or energy transfer that can be monitored by photodetectors such as a CCD spectrometer or a digital camera. This approach was applied with complementary ex situ experiments to examine the aerobic oxidation of anthracene with tris(2,2′-bipyridine)ruthenium(II) as the catalyst. The reaction results in the precipitation of an isometrically pure *syn*-tetraepoxide not seen in prior studies when an organic photocatalyst was employed. Changes in the emission were observed not only upon electron/energy transfer quenching of the catalyst but also from the presence of particles (undissolved substrate and precipitated product). These features impart dissimilar spectral distributions that can be discriminated by their relative contributions to the RGB data of the digital images. The approach thus enables interrogation of multiple facets of the reaction for monitoring and optimization, and offers unique insight into the mechanisms of photoredox catalysis systems.

The energy of visible light is generally insufficient to break chemical bonds by direct photoexcitation, but can excite a suitable catalyst to induce electron or energy transfer, which has been exploited for myriad chemical transformations.[1] The most commonly employed photoredox catalysts are Ru(II) and Ir(III) complexes that attain metal-to-ligand charge transfer excited states upon absorption of light in the region 400–450 nm (Figure S1). Electron transfer between the excited catalyst and a substrate, intermediate or sacrificial additive forms the reduced or oxidized catalyst and subsequent reaction completes the catalytic cycle. Reaction selectivity can therefore be 'tuned' through choice of catalyst, based on ground and excited state redox potentials.[1d] Transformations can also be driven by energy transfer from the photo-excited catalyst to access excited triplet states.[2] Moreover, the redox chemistry can be extended beyond the potentials of the catalyst by exploiting energy transfer to an intermediary species such as pyrene or anthracene that then undergoes electron transfer with the substrate.[3]

Most metal complexes utilized for photoredox catalysis are also luminescent, where the radiative deactivation of the excited state competes with energy/electron transfer.[4] This is routinely used in investigations of reaction mechanism[1g] and exploited for the accelerated discovery of new reactions,[5] in which putative quenchers are evaluated with one or more catalysts. In these studies, selected aspects of the synthetic transformation were explored ex situ, using a spectrophotometer lamp as an alternative excitation source. The quenching of the catalyst's luminescence, however, is inherent to its action. Cismesia and Yoon[6] showed that chain processes in photoredox reactions could be characterized by a combination of luminescence quenching and quantum yield measurements. The synthetic transformation was performed in a cuvette within a spectrofluorometer. The reactions were much slower than those under typical photoredox catalysis conditions due to the low intensity of the excitation source. Similarly, Lupton et al.[7] continuously monitored the fluorescence of a single immobilized organic photoredox catalyst in an examination of the consecutive photoelectron transfer[8] mechanism.

Herein we examine in situ luminescence measurements as a direct, continuous probe of photoredox catalysis under typical synthetic reaction conditions. To demonstrate the approach, we selected the aerobic oxidation of anthracene in acetonitrile using the [Ru(bpy)3]2+ catalyst irradiated with blue light, based on the prior work by Fukuzumi et al.[9] using an organic photocatalyst (Figure 1a). The emission profile is shown to provide real-time information on the influence of reaction conditions on features such as dissolution of saturated

[a] Dr. D. J. Hayne,+ Dr. S. Mohapatra,+ J. C. Bawden, Dr. J. L. Adcock, Dr. G. J. Barbante, C. L. Fraser, Dr. T. U. Connell, Prof. P. S. Francis
School of Life and Environmental Sciences
Faculty of Science, Engineering and Built Environment
Deakin University, Geelong, Victoria 3220 (Australia)
E-mail: paul.francis@deakin.edu.au
[b] Dr. E. H. Doeven
Centre for Regional and Rural Futures
Faculty of Science, Engineering and Built Environment
Deakin University, Geelong, Victoria 3220 (Australia)
[c] Prof. J. M. White
School of Chemistry and Bio21 Molecular Science and Biotechnology Institute
The University of Melbourne, Victoria 3010 (Australia)
[d] Prof. L. C. Henderson
Institute for Frontier Materials
Deakin University, Geelong, Victoria 3220 (Australia)
E-mail: luke.henderson@deakin.edu.au
[e] Dr. S. Mohapatra+
School of Physical and Chemical Sciences
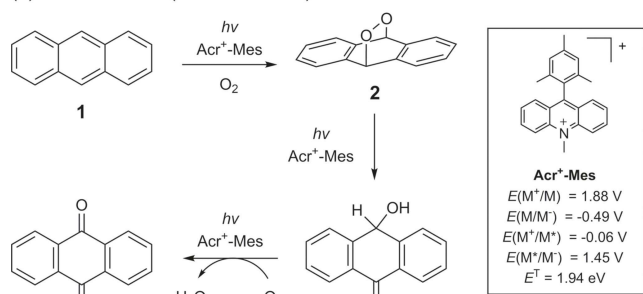Central University of South Bihar, Gaya-824236 (India)
[f] Dr. G. J. Barbante
Land Division, Defence Science and Technology Group
Fishermans Bend, Melbourne, Victoria 3207 (Australia)
[g] Dr. T. U. Connell
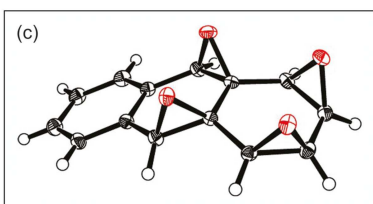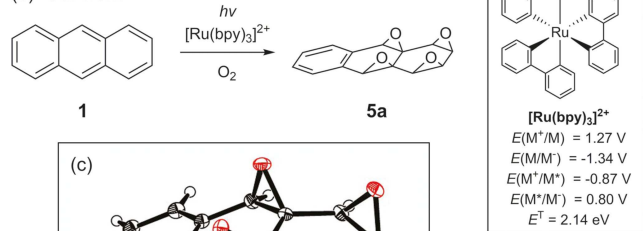School of Science, RMIT University
Melbourne, VIC 3000 (Australia)
[+] These authors contributed equally to this work.
Supporting information for this article is available on the WWW under https://doi.org/10.1002/cptc.201900201

(a) Previous work (Fukuzumi *et al.*)

Acr⁺-Mes
$E(M^+/M) = 1.88$ V
$E(M/M^-) = -0.49$ V
$E(M^+/M^*) = -0.06$ V
$E(M^*/M^-) = 1.45$ V
$E^T = 1.94$ eV

(b) Our work

[Ru(bpy)₃]²⁺
$E(M^+/M) = 1.27$ V
$E(M/M^-) = -1.34$ V
$E(M^+/M^*) = -0.87$ V
$E(M^*/M^-) = 0.80$ V
$E^T = 2.14$ eV

(c)
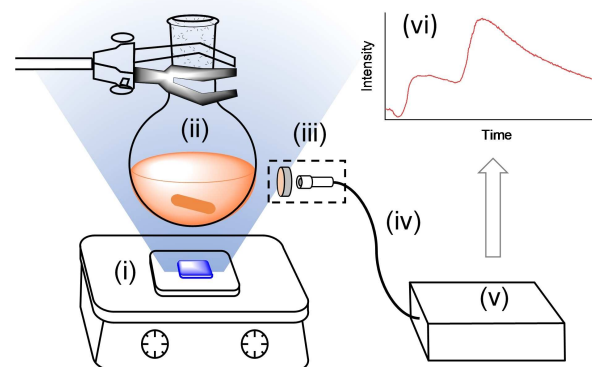
Figure 1. (a) The aerobic oxidation of anthracene (**1**) to anthraquinone (**4**) using 9-mesityl-10-methylacridinium ion (Acr⁺-Mes) as a photoredox catalyst.[9] (b) The aerobic oxidation of anthracene under the conditions of this study to form a *syn*-tetraepoxide (**5a**) using [Ru(bpy)₃]²⁺ as a photoredox catalyst. The catalysts are shown on the right with their ground and triplet excited state reduction potentials (*vs* SCE) and triplet excited state energies.[10] (c) ORTEP representation of **5a**. Thermal ellipsoids set at 50% probability.

Figure 2. Simple configuration to monitor the luminescence of the catalyst over the course of the reaction: (i) LED source light ($\lambda_{max} = 455$ nm) mounted on a magnetic stirrer; (ii) reaction mixture; (iii) long-pass optical filter and collimating lens; (iv) optical fiber; (v) CCD spectrometer; (vi) luminescence intensity over time profile at a selected wavelength (620 nm). The reaction was performed in a fume hood and shielded from room light.
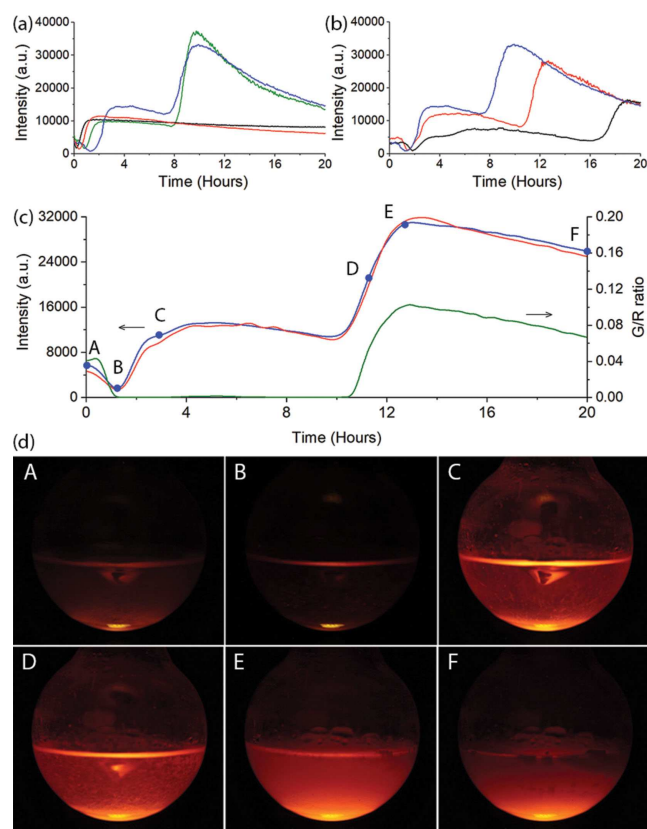
Figure 3. (a) Emission intensity at 620 nm over the course of the aerobic oxidation of anthracene (19 mM = black; 38 mM = red; 57 mM = green; 76 mM = blue) using [Ru(bpy)₃]²⁺ photocatalyst (0.6 mM) in acetonitrile upon irradiation with blue light ($\lambda_{max} = 455$ nm). (b) Intensity at 620 nm from the reaction upon irradiation with the source light at 2.3 W (black line), 3.3 W (red line) or 4.3 W (blue line). (c) Intensity profiles obtained using the CCD detector (620 nm; red line) and luminance data extracted from a selected region of the digital photos (blue line) from the same reaction; and the ratio of the G to R data of the photos (green line) showing the presence of solid starting material at the beginning of the reaction and precipitation of product. (d) Photographs (taken through a 560 nm long-pass filter) of the vessel at the time points shown in Figure 3c.

reactants, formation or consumption of the key chemical species that undergo electron or energy transfer with the catalyst, and precipitation of products. In conjunction with complementary ex situ experiments, the time-resolved luminescence profile provides insight into the reaction mechanism, and opportunities to selectively isolate synthetic intermediates.

Luminescence emanating from the reaction mixture was measured with a charge-coupled device (CCD) spectrometer by mounting an optical fiber with collimating lens at the side of the reaction vessel (Figure 2). In selected experiments, we simultaneously captured the emission using a digital camera (with photographs taken at 5 min intervals). In both cases, a long-pass optical filter was used to block the intense blue excitation light from the photodetector.

Anthracene is sparingly soluble in acetonitrile and at the initiation of the reaction, a considerable portion remained suspended in the stirred solution. The luminescence profile at 620 nm measured upon irradiation of 19 mM anthracene and 0.58 mM [Ru(bpy)₃]²⁺ photocatalyst showed an initial quenching before a rise in intensity that plateaued after ~1 h (Figure 3a, black line). Increasing the concentration of anthracene lengthened the initial quenching time, and at 56 mM and above, a large increase in intensity was observed between 7–10 h, followed by a decrease for the remainder of

the reaction (Figure 3a). The intensity and timing of the luminescence profile features were to an extent dependent on the geometry of the reaction vessel, and could be readily manipulated through the intensity of the source light (Figure 3b). In all cases, the mixture became homogeneous during the early quenching phase and when the large increase in emission intensity was observed, a precipitate had formed. To our surprise, this isolated product was identified as a *syn*-tetraepoxide (**5a**; Figure 1b,c).

Increasing the concentration of the starting material to 250 mM raised the yield of **5a** from 18% to 33% (Table S1 and Figure S2), but also elicited co-precipitation of the corresponding *anti*-tetraepoxide isomer and anthraquinone (**4**). Varying the catalyst concentration did not improve the yield, and no reaction was observed without catalyst or irradiation.

Despite extensive investigations of the oxidation of **1**[9,11] and reactions of **2**, including its isomerization to diepoxide **7** (Figure 4),[12] the only prior reports of **5a** and the corresponding
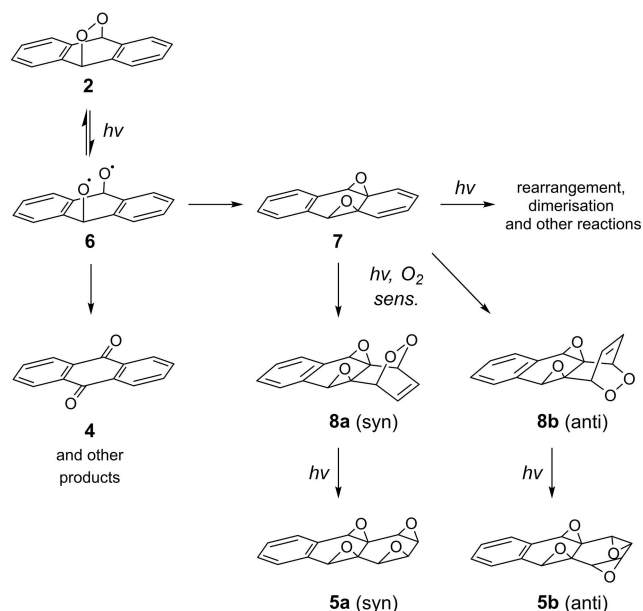

Figure 4. Photooxidation of **2** to form tetraepoxides **5a** and **5b**.[13]

anti-tetraepoxide **5b** were made by Rigaudy et al.[13] in their examination of the many photooxidation intermediates and products of **2** in benzene. As shown in Figure 4, the tetraepoxides (**5a,b**) were formed via **7** and epidioxydiepoxides **8a,b**. Drawing from these studies[13] and the organic photoredox catalysis investigation of Fukuzumi et al.,[9] the features of the emission profiles provide great insight. Epidioxides such as **2** are often formed by photosensitized cycloaddition of singlet oxygen onto the aromatic substrate,[14] for which [Ru(bpy)$_3$]$^{2+}$ is a suitable sensitizer. Fukuzumi et al., however, presented evidence of a photoredox cycle in which the excited Acr$^+$-Mes catalyst oxidizes **1** and then reduces O$_2$, with subsequent radical coupling to form **2**.[9] Unlike Acr$^+$-Mes*, the excited [Ru(bpy)$_3$]$^{2+}$* cannot directly oxidize **1** ($E_{ox}=1.19$ V *vs* SCE).[15] It can, however, transfer energy to attain the triplet excited state

of **1** ($E^T=1.84$ eV),[16] from which electron transfer is then favorable (a variation of the recently described sensitization-initiated electron transfer process[3]). The initial strong quenching of the luminescence by **1** (points A and B in Figure 3c, for example) is indicative of the sensitization-electron transfer pathway. In deaerated acetonitrile, the excited triplet anthracene undergoes annihilation, leading to dimers that can precipitate from solution.[17] In aerated solution, however, dimer formation is completely suppressed,[17] providing further evidence of the efficient generation of **2** via photosensitization coupled with photoredox catalysis. This initial period of quenching is prolonged by an increase in anthracene concentration (Figure 3a), particularly as the rate of reaction is limited by the solubility of the starting material.

The greatest concentration of **2** is therefore expected near point C in Figure 3c, and by stopping the reaction at that time, we were able to selectively isolate this intermediate (details are provided in the Supporting Information). Fukuzumi et al.[9] showed that in the oxidation of **1** catalyzed by Acr$^+$-Mes, **2** was also oxidized by the photoexcited catalyst leading to anthraquinone (**4**) (Figure 1a). However, [Ru(bpy)$_3$]$^{2+}$ is considerably less oxidative. Steady-state luminescence quenching experiments showed that unlike **1**, the isolated intermediate **2** did not quench the photocatalyst emission (Figure S3). The absence of this pathway promotes the photochemical rupture of the peroxide bond of **2** under prolonged irradiation (including the plateau in luminescence intensity after point C).[12a] The biradical intermediate **6** generated by this process can rearrange to **7** (leading to tetraepoxides **5a,b**)[18] or generate products such as **4**.[19] These products do not quench the photocatalyst (Figure S3). The increase in the measured emission intensity to point E in Figure 3c was ascribed to the scattering of light by the precipitated product suspended in solution, and the subsequent decrease (through point F) to the accumulation of product at the base of the vessel.[20] Photography confirmed the times at which solid starting material or product were present (see Figure 3d and the Movie in the Supporting Information).

The scattered light from the particles and the luminescence from the catalyst in homogeneous solution elicited dissimilar spectral distributions. The two phenomena could therefore be discriminated by their relative contributions to the RGB data without visual inspection of the images (in Figure 3c, the green line shows G/R color ratio, which shows the features of the plot corresponding to particles in solution). Several aspects of the reaction described above were verified by analyzing samples taken from the solution over the course of the reaction by HPLC whilst continually monitoring the luminescence of the catalyst, when applying a lower intensity of light to reduce the rate of photochemical steps (details are provided in the Supporting Information).

Under these conditions, a fortuitous balance of activation energy, concentration and solubility allows the isolation of isometrically pure tetraepoxide **5a**, presenting a surprisingly unique entry into the extensive catalogue of studies investigating the formation and fate of epidioxy compounds.[12c,14] This study introduces a new approach to monitor transformations in

These are not the final page numbers! ↗↗

which the key chemical step involves direct reaction with the photoexcited catalyst (rather than the product of its oxidative or reductive quenching). It provides insight into not only energy/electron transfer events but also the depletion or formation of particulates in solution, utilizing inexpensive equipment that is adaptable to most reaction setups.

Experimental Section

Synthesis of *syn*-tetraepoxide 5a

Using the configuration shown in Figure 2, a mixture of anthracene (134 mg, 0.75 mmol) and $[Ru(bpy)_3](PF_6)_2$ (21 mg, 0.024 mmol, 0.8 mol%) in acetonitrile (40 mL) was stirred and irradiated using a blue LED ($\lambda_{max} = 455$ nm), whilst being shielded from ambient light. After 20 h, the reaction mixture was filtered and the collected precipitate washed with a minimum of cold acetonitrile before drying *in vacuo* affording a white powder (50 mg, 0.21 mmol, 28%). ^{1}H-NMR (400 MHz; [CD_3CN]): δ 7.74–7.70 (m, AA′BB′, 2H, C^2H), 7.53-7.48 (m, AA′BB′, 2H, C^1H), 4.18 (s, 2H, C^4H), 3.73-3.71 (m, AA′BB′, 2H, C^7H), 3.15–3.13 (m, AA′BB′, 2H, C^6H). ^{13}C{^{1}H}-NMR (101 MHz; [CD_3CN]): δ 132.7 (2 C, C^3), 131.8 (2 C, C^2), 130.6 (2 C, C^1), 58.8 (2 C, C^4), 55.0 (2 C, C^6), 54.8 (2 C, C^5), 50.2 (2 C, C^7). ESI-MS (positive ion). Calcd for $C_{14}H_{11}O_4^+$ ([M+H]$^+$): *m/z* 243.065. Found *m/z* 243.0671. X-ray crystallography details are in the Supporting Information and Deposition Number 1943031 contains the supplementary crystallographic data for this paper. These data are provided free of charge by the joint Cambridge Crystallographic Data Centre and Fachinformationszentrum Karlsruhe Access Structures service www.ccdc.cam.ac.uk/structures.

Spectrometer

The light emanating from the reaction vessel was measured using an Ocean Optics QE65 Pro charge coupled device (CCD) spectrometer via optical fibre (1 m length, 1 mm core diameter), collimating lens (74-UV, 200–2000 nm, Ocean Optics), and long-pass optical filter (540LP RapidEdge, Omega Optical), which were mounted near the side of the reaction vessel using an in-house fabricated holder. The spectrometer was operated and data were recorded using OceanView software. Emission profiles were processed with an FFT filter using Origin software to remove noise.

Photographs

A Canon 6D Camera, with Tokina 100 mm f2.8 AT-X PRO Macro lens was mounted on a tripod next to the reaction vessel. The camera was powered using a Glorich ACK-E6 Replacement AC Power Adapter Kit. A long-pass optical filter was positioned in front of the lens using an in-house fabricated holder. Various optical filters were tested (*e.g.* Figure S4). A 560 nm long-pass filter was used for the images shown in Figure 3, and those used to create the time-lapse movie, which was compiled with Adobe Premier Pro 2019 software. Emission profiles were extracted from a selected region of the time-lapse movie using Tracker 5.0.7 software (https//physlets.org/tracker).

Conflict of Interest

The authors declare no conflict of interest.

[1] a) J. Xuan, W.-J. Xiao, *Angew. Chem. Int. Ed.* **2012**, *51*, 6828–6838; *Angew. Chem.* **2012**, *124*, 6934–6944; b) C. K. Prier, D. A. Rankic, D. W. C. MacMillan, *Chem. Rev.* **2013**, *113*, 5322–5363; c) Y. Xi, H. Yi, A. Lei, *Org. Biomol. Chem.* **2013**, *11*, 2387–2403; d) T. Koike, M. Akita, *Inorg. Chem. Front.* **2014**, *1*, 562–576; e) R. A. Angnes, Z. Li, C. R. D. Correia, G. B. Hammond, *Org. Biomol. Chem.* **2015**, *13*, 9152–9167 ; f) G. Duret, R. Quinlan, P. Bisseret, N. Blanchard, *Chem. Sci.* **2015**, *6*, 5366–5382; g) D. M. Arias-Rotondo, J. K. McCusker, *Chem. Soc. Rev.* **2016**, *45*, 5803–5820; h) I. Ghosh, L. Marzo, A. Das, R. Shaikh, B. Koenig, *Acc. Chem. Res.* **2016**, *49*, 1566–1577.

[2] a) Z. Lu, T. P. Yoon, *Angew. Chem. Int. Ed.* **2012**, *51*, 10329–10332; *Angew. Chem.* **2012**, *124*, 10475–10478; b) T. R. Blum, Z. D. Miller, D. M. Bates, I. A. Guzei, T. P. Yoon, *Science* **2016**, *354*, 1391–1395; c) N. Münster, N. A. Parker, L. v. Dijk, R. S. Paton, M. D. Smith, *Angew. Int. Ed.* **2017**, *56*, 9468–9472; *Angew. Chem.* **2017**, *129*, 9596–9600; d) F. M. Hörmann, T. S. Chung, E. Rodriguez, M. Jakob, T. Bach, *Angew. Chem. Int. Ed.* **2018**, *57*, 827–831; *Angew. Chem.* **2018**, *130*, 835–839.

[3] a) C. Kerzig, M. Goez, *Chem. Sci.* **2016**, *7*, 3862–3868; b) I. Ghosh, R. S. Shaikh, B. König, *Angew. Chem. Int. Ed.* **2017**, *56*, 8544–8549; *Angew. Chem.* **2017**, *129*, 8664–8669.

[4] a) G. J. Barbante, N. Kebede, C. M. Hindson, E. H. Doeven, E. M. Zammit, G. R. Hanson, C. F. Hogan, P. S. Francis, *Chem. Eur. J.* **2014**, *20*, 14026–14031; b) E. H. Doeven, E. M. Zammit, G. J. Barbante, P. S. Francis, N. W. Barnett, C. F. Hogan, *Chem. Sci.* **2013**, *4*, 977–982; c) E. Kerr, E. H. Doeven, G. J. Barbante, C. F. Hogan, D. Bower, P. S. Donnelly, T. U. Connell, P. S. Francis, *Chem. Sci.* **2015**, *6*, 472–479.

[5] a) M. N. Hopkinson, A. Gomez-Suarez, M. Teders, B. Sahoo, F. Glorius, *Angew. Chem. Int. Ed.* **2016**, *55*, 4361–4366; *Angew. Chem.* **2016**, *128*, 4434–4439; b) K. P. L. Kuijpers, C. Bottecchia, D. Cambié, K. Drummen, N. J. König, T. Noël, *Angew. Chem. Int. Ed.* **2018**, *57*, 11278–11282; *Angew. Chem.* **2018**, *130*, 11448–11452.

[6] M. Cismesia, T. Yoon, *Chem. Sci.* **2015**, *6*, 5426–5434.

[7] J. Haimerl, I. Ghosh, B. Koenig, J. Vogelsang, J. M. Lupton, *Chem. Sci.* **2019**, *10*, 681–687.

[8] I. Ghosh, T. Ghosh, J. I. Bardagi, B. König, *Science* **2014**, *346*, 725–728.

[9] H. Kotani, K. Ohkubo, S. Fukuzumi, *J. Am. Chem. Soc.* **2004**, *126*, 15999–16006.

[10] a) A. C. Benniston, A. Harriman, P. Li, J. P. Rostron, H. J. Van Ramesdonk, M. M. Groeneveld, H. Zhang, J. W. Verhoeven, *J. Am. Chem. Soc.* **2005**, *127*, 16054–16064; b) Y. Kawanishi, N. Kitamura, S. Tazuke, *Inorg. Chem.* **1989**, *28*, 2968–2975; c) S. Fukuzumi, H. Kotani, K. Ohkubo, S. Ogo, N. V. Tkachenko, H. Lemmetyinen, *J. Am. Chem. Soc.* **2004**, *126*, 1600–1601.

[11] a) M. Klaper, P. Wessig, T. Linker, *Chem. Commun.* **2016**, *52*, 1210–1213; b) S. Fukuzumi, I. Nakanishi, K. Tanaka, *J. Phys. Chem. A* **1999**, *103*, 11212–11220; c) S. L. H. Rebelo, M. M. Q. Simoes, M. G. P. M. S. Neves, A. M. S. Silva, J. A. S. Cavaleiro, *Chem. Commun.* **2004**, 608–609; d) T. Devi, Y.-M. Lee, W. Nam, S. Fukuzumi, *Chem. Commun.* **2019**, DOI: 10.1039/c9cc03245b.

[12] a) J. Rigaudy, A. Defoin, J. Baranne-Lafont, *Angew. Chem. Int. Ed.* **1979**, *18*, 413–415; *Angew. Chem.* **1979**, *91*, 443–444; b) R. Schmidt, H.-D. Brauer, *J. Photochem.* **1986**, *34*, 1–12; c) H. Fidder, A. Lauer, W. Freyer, B. Koeppe, K. Heyne, *J. Phys. Chem. A* **2009**, *113*, 6289–6296; d) B. Siret, S. Albrecht, A. Defoin, *C. R. Chim.* **2014**, *17*, 1075–1079; e) M. Bauch, M. Klaper, T. Linker, *J. Phys. Org. Chem.* **2017**, *30*, e3607; f) W. Fudickar, T. Linker, in *The Chemistry of Peroxides, Vol. 3* (Eds.: A. Greer, J. F. Liebman), John Wiley & Sons, Chichester, England, **2014**, pp. 21–86.

[13] a) A. Defoin, J. Baranne-Lafont, J. Rigaudy, *Bull. Soc. Chim. Fr.* **1984**, 145–155; b) J. Rigaudy, J. Baranne-Lafont, A. Ranjon, A. Caspar, *Bull. Soc. Chim. Fr.* **1984**, 187–194.

[14] J.-M. Aubry, C. Pierlot, J. Rigaudy, R. Schmidt, *Acc. Chem. Res.* **2003**, *36*, 668–675.

[15] S. Fukuzumi, K. Ohkubo, T. Okamoto, *J. Am. Chem. Soc.* **2002**, *124*, 14147–14155.

[16] M. Wrighton, J. Markham, *J. Phys. Chem. C* **1973**, *77*, 3042–3044.

[17] R. R. Islangulov, F. N. Castellano, *Angew. Chem. Int. Ed.* **2006**, *45*, 5957–5959; *Angew. Chem.* **2006**, *118*, 6103–6105.

[18] F. Sevin, M. L. McKee, *J. Am. Chem. Soc.* **2001**, *123*, 4591–4600.

[19] S. Dong, A. Ong, C. Chi, *J. Photochem. Photobiol. C* **2019**, *38*, 27–46.

[20] N. Yoshikawa, H. Kimura, S. Yamabe, N. Kanehisa, T. I. Takashima, *J. Mol. Struct.* **2016**, *1117*, 49–56.

These are not the final page numbers! ↗↗

COMMUNICATIONS

Capturing the light: Monitoring photoredox catalysis systems with a simple photodetector such as a miniaturized spectrometer or a digital camera reveals the timeframe of key electron/energy transfer quenching events and the dissolution and precipitation of solids. This approach is applied to the aerobic oxidation of anthracene with tris(2,2′-bipyridine) ruthenium(II) as the catalyst, which yields an isometrically pure *syn*-tetraepoxide.
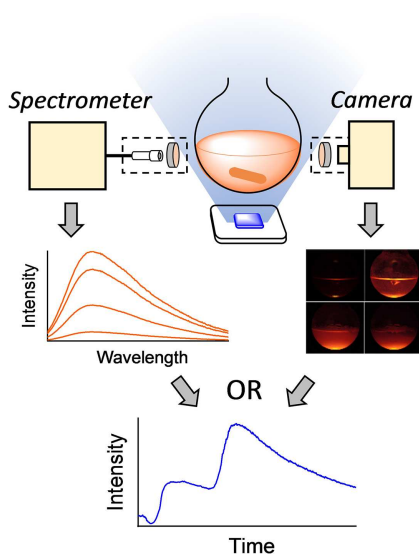
Dr. D. J. Hayne, Dr. S. Mohapatra, J. C. Bawden, Dr. J. L. Adcock, Dr. G. J. Barbante, Dr. E. H. Doeven, C. L. Fraser, Dr. T. U. Connell, Prof. J. M. White, Prof. L. C. Henderson*, Prof. P. S. Francis*

1 – 6

Catalyst Luminescence Exploited as an Inherent In Situ Probe of Photoredox Catalysis